Isolated ultracold porphyrins in supersonic expansions. III. Freebase porphine

Article *in* The Journal of Chemical Physics · November 1982

DOI: 10.1063/1.444440

2 authors:

Uzi Even
Tel Aviv University
194 PUBLICATIONS **6,884** CITATIONS
SEE PROFILE

Joshua Jortner
Tel Aviv University
802 PUBLICATIONS **41,292** CITATIONS
SEE PROFILE

Isolated ultracold porphyrins in supersonic expansions. III. Freebase porphine

Uzi Even and Joshua Jortner

Citation: The Journal of Chemical Physics **77**, 4391 (1982); doi: 10.1063/1.444440
View online: http://dx.doi.org/10.1063/1.444440
View Table of Contents: http://scitation.aip.org/content/aip/journal/jcp/77/9?ver=pdfcov
Published by the AIP Publishing

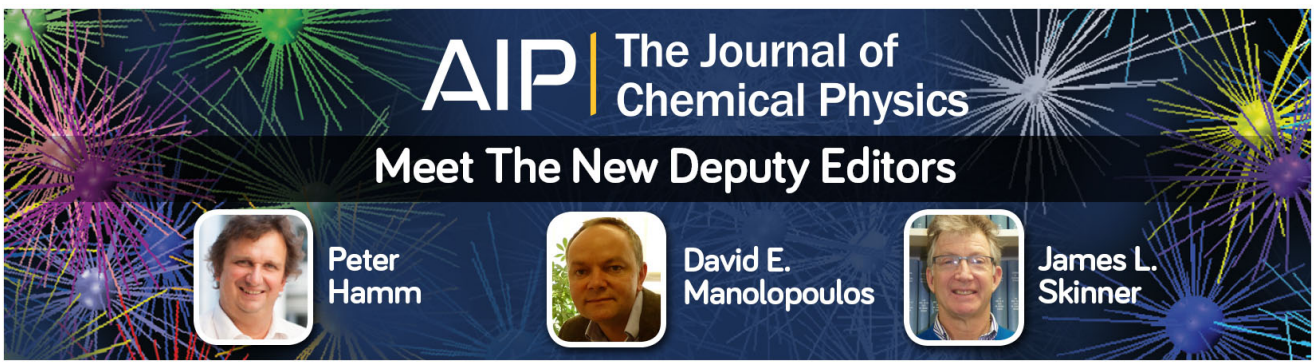

Isolated ultracold porphyrins in supersonic expansions. III. Free-base porphine

Uzi Even and Joshua Jortner

Department of Chemistry, Tel-Aviv University, Tel Aviv, Israel
(Received 3 May 1982; accepted 24 June 1982)

The vibrational level structure of the $S_0 \rightarrow S_1^x$ transition (the Q_x band) and of the $S_0 \rightarrow S_1^y$ transition (the Q_y band) of free-base porphine in supersonic expansions of He was interrogated by laser-induced fluorescence excitation spectroscopy. Electronic relaxation in the S_1^x manifold was explored by time-resolved spectroscopy, revealing a constant value of the decay lifetime $\tau = 9.5 \pm 1.0$ ns for excess vibrational energies in the range $E_v = 0$–5000 cm^{-1}. The line broadening (FWHM) $\Delta = 1.0$–1.5 cm^{-1} of the electronic origin and of low-lying vibrational excitations in the S_1^x manifold originates from inhomogeneous unresolved rotational structure, while the large linewidth $\Delta = 11.9$ cm^{-1} of the electronic origin of the S_1^y state is due to homogeneous electronic relaxation broadening in the statistical limit. The line shape of the electronic origin of S_1^y was found to be Lorentzian, providing a quantitative determination of the lifetime $\tau = 5 \times 10^{-13}$ s for interstate S_1^y–S_1^x electronic relaxation within a bound level structure of a large isolated molecule.

I. INTRODUCTION

In this work we continue our spectroscopic studies[1–6] of excited-state energetics and dynamics of porphyrins in pulsed supersonic expansions of He, reporting on the results of an experimental study of energy-resolved and time-resolved laser spectroscopy of the free-base porphine(H_2P) molecule. From the spectroscopic point of view, H_2P is the most important porphyrin. We have studied the $S_0 - S_1^x$ transition (the Q_x band)[7–11] and the $S_0 - S_1^y$ transition (the Q_y band)[7,11] of the isolated H_2P. A preliminary report of this study, which focused attention on intramolecular interstate relaxation phenomena has already been published.[3] In what follows we shall provide information on the electronic level structure, vibrational level structure, electronic relaxation from the lowest excited S_1^x state, as interrogated by time-resolved spectroscopy, and electronic relaxation from the S_2^y state, as explored by spectroscopic Lorentzian line broadening.

II. EXPERIMENTAL DETAILS

The experimental techniques for laser spectroscopy in pulsed, seeded, supersonic expansions were described previously.[2,4] A solid sample of H_2P (commercially obtained from Porphyrin Products) was heated in the nozzle chamber to 320–380 °C. The vapor pressure of H_2P at 330 °C is 0.2 Torr.[11] In contrast to the features of "floppy" tetraphenylporphyrins,[1,4] we found that effective cooling of H_2P, without extensive complex formation, could be accomplished in Ar over a narrow range of the stagnation pressure p, as is the case for other "rigid" molecules. The H_2P molecule could effectively be cooled in supersonic expansions of Ar at the stagnation pressures $p = 100$–150 Torr, as well as in supersonic jets of He expanded at $p = 1500$–2500 Torr, with the nozzle diameter being $D = 600$ μm. We have demonstrated that the laser-induced fluorescence (LIF) spectra obtained under these conditions exhibit the electronic-vibrational excitations of the bare H_2P molecule, rather than rare-gas-H_2P van der Waals (vdW) complexes, as practically identical spectra were obtained in Ar and in He. No evidence was obtained for the formation of He-H_2P vdW complexes under our experimental conditions. Spectroscopic evidence for the formation of Ar_n-H_2P vdW complexes was obtained in Ar expansions at $p = 150$–1500 Torr, which will be reported elsewhere.[12] The spectroscopic studies of the bare H_2P molecule, reported herein, were conducted in jets of He.

A serious question arising in relation to spectroscopy of porphyrins in supersonic expansions is whether the LIF spectrum is not contaminated by thermal decomposition products. The pioneering studies of Hochstrasser *et al.*[13] and Gouterman and his colleagues[11,13,14,15] provided comforting evidence regarding the thermal stability of many porphyrins[11,13,14] and related compounds[15] in the gas phase at elevated temperatures, where the vapor pressure of the large molecule is ~0.1 Torr. The thermal stability of many porphyrins makes them amenable to exploration in seeded supersonic expansions.[1–5,16] However, extreme care must be exerted to avoid pitfalls due to thermal decomposition products of porphyrins, which will result in alien spectral features in the LIF spectra of the seeded expansions. Concerning H_2P, which is the subject matter of the present study, Gouterman *et al.*[11] have shown that heating this molecule to about ~390 °C resulted in the appearance of a spectral band at 6420 Å, which was attributed[11] to free-base chlorine (H_2Chl). We have demonstrated that the LIF spectra of H_2P in supersonic expansions, produced at a nozzle temperature of 330 °C, did not change and did not exhibit new spectral features after maintaining the nozzle at 330 °C for 8 h. We concluded that under these operating conditions at 330 °C the spectrum is free from thermal decomposition products. Heating the nozzle to 370 °C resulted in the appearance of a "new spectrum," which appears together with the spectral features of H_2P and whose origin is red shifted relative to the origin of the $S_0 - S_1^x$ transition of H_2P. According to the vibrational analysis performed in Sec. IV, this "new spectrum", resulting from thermal decomposition of H_2P, is attributed to H_2Chl, being in accord with the original observation of Gouterman *et al.*[11] At $T = 330$ °C our spectra of H_2P were found to be practically free from the H_2Chl impurity.

 021-9606/82/214391-09$02.10

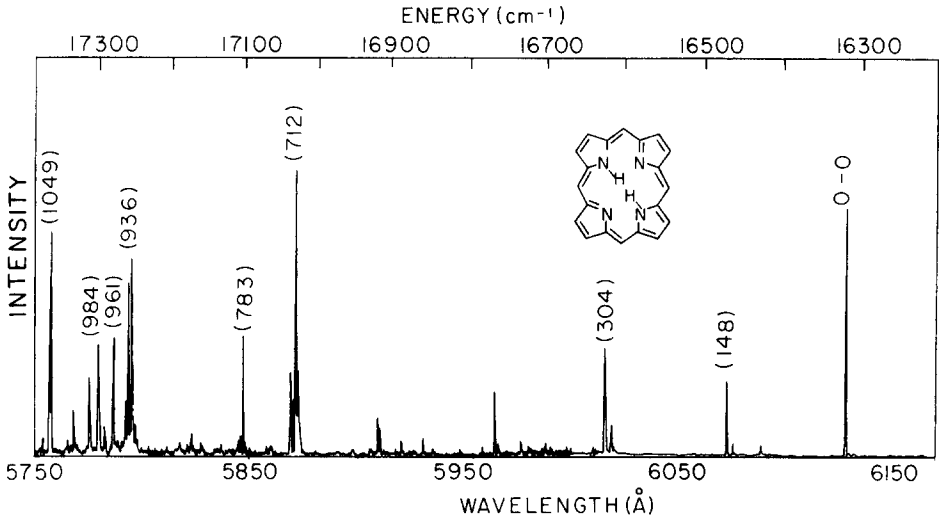

FIG. 1. Fluorescence excitation spectrum in the region 5750–6160 Å of H_2P in pulsed supersonic expansions of He. H_2P was heated in the nozzle chamber to 330°C, seeded in He at $p = 2000$ Torr and expanded through the 600 μm nozzle. The exciting dye laser crossed the jet at 12 cm down the nozzle. The intensity in the range 6000–6150 Å is higher by a numerical factor of 3 than the intensity in the range 5750–6000 Å. The electronic origin of the $S_0 \rightarrow S_1^x$ transition is marked 0–0, while fundamental vibrational excitations above the origin (in cm^{-1}) are marked by numbers in brackets.

III. THE $S_0 \rightarrow S_1^x$ TRANSITION

Figures 1 and 2 show the fluorescence excitation spectrum in the range 5550–6160 Å of H_2P cooled in supersonic expansions of He. This spectrum is attributed to the lowest spin-allowed $S_0 \rightarrow S_1^x$ transition. No intrinsic spectral features of the bare H_2P molecule could be observed in the wavelength region above 6160 Å. The lowest energy, intense, spectral feature of 6127.5 Å (16320 cm^{-1}) is assigned to the electronic origin 0–0 of the $S_0 \rightarrow S_1^x$ transition. The linewidth of the 0–0 transition is $\Delta = 1.0$ cm^{-1} (at $p = 2000$ Torr He), being due to unresolved rotational structure. The line shape was symmetric in contrast to the asymmetric envelope function for the 0–0 $S_0 \rightarrow S_1$ transition of Zn-tetrabenzoporphyrin.[5] In Table I the characteristics of the electronic origin of the Q_x band of the isolated ultracold molecule are confronted with those of the gas phase,[11] solution,[11] and Shpolskii crystal[9] spectra, demonstrating again the remarkable simplification and high resolution accomplished by the present approach. From Table I it is evident that the solvent shifts for the electronic origin of the $S_0 \rightarrow S_1^x$ transition are rather small, being about -112 cm^{-1} for benzene. For the $\pi\pi^*$ transition of H_2P, which exhibits only a minor charge expansion in the excited state, one expects that dispersive interactions will dominate the spectral shift. As the $S_0 \rightarrow S_1^x$ transition of H_2P is characterized by a low oscillator strength $f \sim 0.01$,[11] one expects a modest dispersive red solvent shift $\delta\nu$ for this transition,[17,18] which is considerably smaller than typical values of $\delta\nu \simeq -500$ cm^{-1} observed for the electronic origin of intense $\pi\pi^*$ transitions with $f \sim 0.1$–0.3.[18] What is intriguing is that the solvent shifts for some trapping sites in Shpolskii crystals[9] (Table II) are positive. Such positive values of $\delta\nu$ were not encountered previously for $\pi\pi^*$ transitions. These may originate from the following causes:

(1) Enhancement of short-range repulsive H_2P medium interactions in the S_1^x state. This effect, which is exhibited for He van der Waals complexes,[18] is expected to be minor for $\pi\pi^*$ excitations.

(2) Intramolecular configurational changes induced by the medium. A medium-induced change in the geometry of the internal N–H bonds is a plausible possibility for such effects, which will modify the energy levels of H_2P. Such a "chemical" mechanism, originally proposed by Gouterman *et al.*,[11] may provide a dominating contribution to $\delta\nu$ for the weak $S_0 \rightarrow S_1^x$ transition, resulting in an overall positive spectral shift.

LIF spectra of large molecules in seeded jets provide extensive and exhaustive information on vibrational level structure in excited electronic states. The vibrational assignment of the $S_0 \rightarrow S_1^x$ transition of the isolated H_2P molecule is given in Table III. The prominent fundamental vibrations were tentatively assigned according to two criteria: (i) High or medium relative intensity and (ii) appearance of combination bands $\omega_1 + \omega_2$, whose relative intensities are roughly $I_1 I_2$, where I_1 and I_2 are the relative intensities of the individual ω_1 and ω_2 vibrational excitations. It is interesting to note that a large number of such combination bands appear in the spectrum. Some additional weak spectral

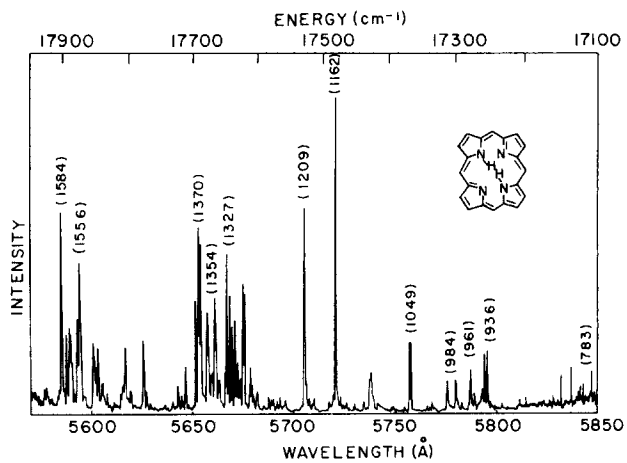

FIG. 2. Fluorescence excitation spectrum in the range 5570–5850 Å of H_2P in pulsed supersonic expansions of He. Experimental conditions as in Fig. 1. Numbers in brackets represent fundamental vibrational excitations (in cm^{-1}).

TABLE I. Energetics of the electronic origin of the $S_0 \rightarrow S_1^x$ transition (the Q_x band) of free-base porphine.

Medium	Peak energy (cm^{-1})	Spectral bandwidth (cm^{-1})	Assignment	Reference
Supersonic expansion of He	16 320	1.0	0–0 Rotational broadening	Present work
Gas phase 393°C	15 974	770	Unresolved vibrational sequence congestion and rotational broadening	11
Benzene solution 25°C	16 200	300	Unresolved vibrational sequence congestion and inhomogeneous broadening	11
n-hexane 2 K	16 396	~3	0–0 Inhomogeneous broadening	9
	16 295	~3	Crystal field splitting of origin	

features, which could not be attributed to combination bands, may also correspond to fundamentals. However, their assignment is uncertain.

The fundamentals in the S_1^x state of H_2P (Table III) may correspond either to totally symmetric vibrations or to vibronically induced false origins; a distinction between these two possibilities cannot be made at present. In addition to the fundamentals and their combination bands, Fermi resonances are exhibited, e.g., the pair of intense lines at 936 and 940 cm^{-1} or the pair at 1049 and 1051 cm^{-1}. In this case, the lower energy component of each pair was arbitrarily labeled as the fundamental. At higher values of the excess vibrational energies E_v in the range $E_v \geq 1300$ cm^{-1}, the vibrational level structure becomes dense and starts to exhibit the spectroscopic manifestations of many-level Fermi resonances.

The vibrational level structure in the S_1^x state of H_2P in a Shpolskii crystal was investigated by Voelker and MacFarlane[19] by the singlesite excitation method. In Table III we compare the vibrational frequencies of the isolated molecule with those of H_2P in *n*-octane at 4.2 K. The only inconsistency between the isolated and the medium perturbed molecule involves the low-frequency 118 cm^{-1} vibrational mode in the crystal, whose counterpart in the isolated molecule may correspond either to the 105 or 140 cm^{-1} vibration. Such low frequency modes, which may presumably involve out-of-plane motion of the ring or, alternatively, the motion of the two H atoms, are expected to be sensitive to medium perturbations. In the energy region $140 < E_v < 1600$ cm^{-1} there is a remarkable correspondence between all 19 vibrational excitations of H_2P observed in *n*-hexane crystal[19] and the isolated-molecule vibrational states in the S_1^x manifold. The largest medium shift of the vibrational modes involves the low frequency 148 ± 2 cm^{-1} mode of the isolated molecule, which is shifted to 155 cm^{-1} in the *n*-hexane crystal. For all the other vibrational excitations in the crystal, the medium shifts are small, being barely within experimental uncertainty. The information concerning the vibrational level structure emerging from the isolated-molecule spectrum is much more detailed than that previously obtained from the Shpolskii crystal spectrum. The isolated-molecule spectrum reveals a large number of weak features as well as some closely spaced intense features, which were not amenable to observation in the mixed crystal spectrum. The spectroscopic resolution of the beautiful technique of site selection excitation spectroscopy[8–10,19] in Shpolskii crystals is inherently limited by two effects. Firstly, inhomogeneous broadening prevails for excitations at each site. Secondly, higher vibrational excitations in the solid may exhibit additional homogeneous line broadening due to medium-induced vibrational excitations, which may occur on the picosecond time scale. The isolated molecule LIF spectra are definitely superior with respect to spectral resolution, their resolution being intrinsically limited by (i) small rotational broadening ($\Delta = 1.0 - 1.5$ cm^{-1} for individual low-lying electronic-vibrational excitations in S_1^x), (ii) spectral congestion in the higher vibrational excitations in S_1^x, which in turn is determined by Δ, and (iii) intramolecular interstate relaxation in higher electronic states (Sec. VI), which results in homogeneous line

TABLE II. Spectral shifts $\delta\nu = \nu_{00}$ (medium) $- \nu_{00}$ (bare molecule) for the electronic origin of H_2P in Shpolskii crystals at 2 K. The energies of the origin ν_{00} (medium) in sites A_1, A_2, B_1, and B_2 are taken from Ref. 9.

	$\delta\nu$ (cm^{-1})			
Medium	Site A_1	Site A_2	Site B_1	Site B_2
n-hexane	+76	−25	...	...
n-heptane	−20	−28	−4	−20
n-octane	+11	−54	−22	−48

TABLE III. Vibrational level structure in the S_1^x state (Q_x band) of free-base porphine. Electronic origin of isolated molecule at 16 320 cm^{-1}.[a]

Isolated molecule in supersonic expansion of He (present work)			Molecule in *n*-octane crystal (Ref. 19)
$\Delta\nu$[b] (cm^{-1})	I[c]	Assignment[d,e]	$\Delta\nu$ (cm^{-1})
0	100	0–0	
105	4		118 (m)
140	5		
148	30	F	155 (s)
296	10	2×148	
304	43	F	308 (s)
448	6	3×148+4 304+148−4	
541	2		
570	1		
598	2	4×148+6 (?)	
602	4	2×304−6	
709	8		
712	28	F	710 (s)
714	5		
719	8		
783	12	F	783 (m)
856	2	712+148−4	
931	3	783+148	
936	18	F	943 (s)
940	14		
944	4		
961	10	F	970 (m)
974	2		
984	9	F	987 (m) (w)
996	6		993 (m) (w)
1017	3	712+304	1018 (w)
1049	18	F	1052 (w)
1051	14		
1090	2	940+148+2	
1108	10	961+148−1	1109 (m)
1162	80	F	1161 (m)
1209	50	F	1210 (m)
1291	11		
1300	8		
1302	32		1297 (s)
1307	7		
1311	12		
1314	22	1162+148+4	
1319	20		
1327	30		
1327	40	F	
1345	25	F	1340 (m)
1351	8	1051+304−4 1049+304−2 1209+148−6	
1354	24	F (?)	1355 (s)
1368	38	F (?)	
1370	40	F (?)	
1375	25		
1391	10		
1403	5		
1456	20	1162+304+10 1302+148+6 1307+148+1	
1485	15	712+783+10 1327+148+10 1345+148−8	1478 (m)
1511	5	1354+148+9 1209+344+2	
1520	7	1368+148+4 1370+148+2	
1527	20	1375+148+2	
1530	12		
1534	22		
1556	50	F (?)	1552 (s)
1560	28		
1568	20		
1571	20		
1577	20		
1584	50	F (?)	1588 (s)

[a]Absolute accuracy of 0–0 position is ±4 cm^{-1}.
[b]$\Delta\nu$—frequencies relative to electronic origin. Accuracy ±2 cm^{-1}.
[c]I—relative peak intensity. Accuracy ±25%.
[d]F—fundamental vibrations.
[e]When pairs of Fermi resonances are exhibited, the lowest frequency component is arbitrarily labeled as the fundamental.

broadening in the isolated molecule. We were able to observe and analyze the vibrational level structure of the $S_0 - S_1^x$ transition up to excess vibrational energies of $E_v = 1600$ cm^{-1}. In the spectral range 5050–5570 Å a "spectroscopic desert" is exhibited, the LIF spectrum being extremely weak and practically devoid of any pronounced structure.

IV. A THERMAL DECOMPOSITION PRODUCT

The spectra produced by heating the H_2P sample in the nozzle chamber to 330 °C were free from thermal

decomposition products. Heating the nozzle to 370–390 °C resulted in the appearance of new spectral features, whose intensity gradually increases when the nozzle is maintained at these elevated temperatures. Figures 3 and 4 demonstrate the appearance of the new spectrum in the energy range below the 6127.5 Å origin of H_2P (Fig. 3) and in the vicinity of the 304 cm^{-1} vibrational excitation of H_2P. These new spectral features, which appear together with the spectral features of H_2P, are obviously due to a thermal decomposition product (TDP) of H_2P. In Table IV we list the positions together with rough estimates of the intensities of the spectral features of the TDP. As no additional discrete spectral features were observed at wavelengths below 6285 Å, we assigned the intense 6284.5 Å to the electronic origin of the TDP. The TDP is identified as the free-base chlorine (H_2Chl) on the basis of the comparison of its vibrational level structure with the vibrational excitations of H_2Chl in a Shpolskii crystal.[19] As is apparent from Table IV, the vibrational level structure of the TDP is practically identical with that of H_2Chl. It will be interesting to compare the vibrational level structure of TDP with H_2P. Three features of the vibrational level structure (Fig. 3) of the TDP should be noted in this context. First, the relative intensity of the 150 cm^{-1} vibration is low in contrast to the intense 148 cm^{-1} vibration of H_2P (Table III). Second, a weak feature at 352 cm^{-1}, which is absent for H_2P. Third, the single intense 710 cm^{-1} feature of H_2P is replaced by the pair 716 and 726 cm^{-1} in the TDP.

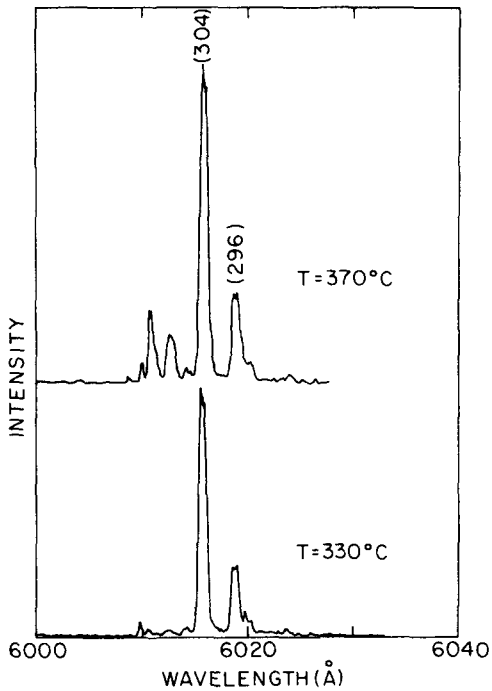

FIG. 4. Fluorescence excitation spectrum of the thermal decomposition product of H_2P in the range 6000–6040 Å. The spectrum produced by heating the nozzle to 330°C (lower curve) reveals the 296 and 304 cm^{-1} vibrational features of H_2P, which are marked by numbers in brackets. Heating the nozzle to 370°C (upper curve) reveals new spectral features of the H_2–chlorine (see the text).

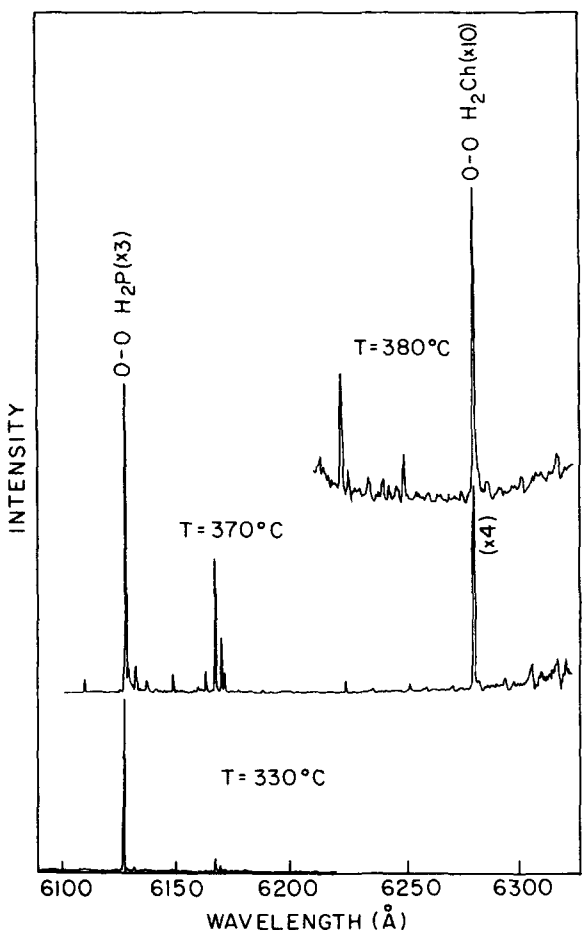

FIG. 3. Fluorescence excitation spectra of the thermal decomposition product of H_2P. The spectrum produced by heating the nozzle chamber to 330°C (lower curve) reveals only very weak features on the long-wavelength side of the electronic origin of H_2P, which is marked 0–0 H_2P. Heating the nozzle to 370 (middle curve) and 380°C (upper curve) reveals the spectrum of the thermal product, which is assigned to H_2-chlorine (see the text), whose origin is marked by 0–0 H_2Chl.

TABLE IV. Fluorescence excitation spectrum of the thermal decomposition spectrum of free-base porphine. Electronic origin of free-base porphine at 6127.5 Å.

Spectrum in supersonic jet		H_2-chlorine in n-hexane crystal (Ref. 19)
Wavelength (Å)	$\Delta\nu$ (cm^{-1})	$\Delta\nu$ (cm^{-1})
6284.5 (s)	0	0–0
6255.0 (vw)	75	
6226.2 (w)	150	152 (w)
6172.0 (w)	290	
6170.1 (m)	295	288 (s)
6168.0 (s)	301	303 (s)
6163.5 (w)	312	
6148.5 (w)	352	355 (vw)
6013.9	716	713 (s)
6010.0	726	721 (s)

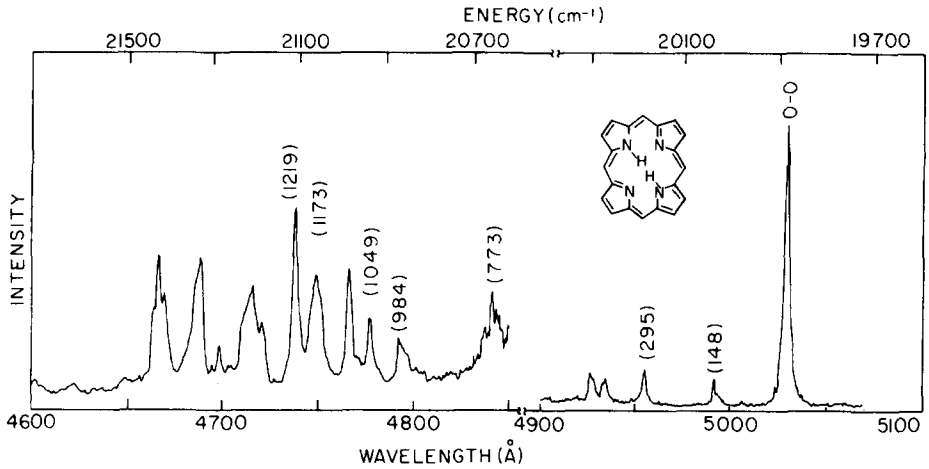

FIG. 5. Fluorescence excitation spectrum in the region 4900–5100 Å of H_2P in pulsed supersonic expansions of He. Experimental conditions as in Fig. 1. The electronic origin of the $S_0 \rightarrow S_1^y$ transition is marked 0–0, while fundamental vibrational excitations are marked by numbers in brackets (in cm^{-1}).

These distinct features of the vibrational level structure of the TDP are exhibited by H_2Chl.[19] We thus conclude that the TDP is H_2Chl, being produced by thermal reduction of H_2P, as originally proposed by Gouterman *et al.*[11] The electronic origin of the $S_0 \rightarrow S_1^x$ transition of the bare H_2Chl molecule is located at 15192 cm^{-1}. The spectral shifts $\delta\nu$ of the electronic origin of H_2Chl in Shpolskii crystals relative to the bare molecule are somewhat larger than those for H_2P. For example, the combination of the crystal data of Voelker and MacFarlane[19] with our assignment of the 0–0 of the S_1^x state of H_2Chl results in the values of -123, -144, -152, and -156 cm^{-1} for the spectral shifts of H_2Chl in the four sites of the *n*-hexane crystal. These red spectral shifts, originating from dispersive interactions, are larger in their absolute values than those for the S_1^x origin of H_2P (discussed in Sec. III). As the oscillator strength of the $S_0 \rightarrow S_1^x$ transition in H_2Chl is higher than for the corresponding transition in H_2P, we expect that in the former case the contribution of dispersive interactions to $\delta\nu$ will be larger,[17,18] providing a dominant contribution to the spectral shift.

V. THE $S_0 \rightarrow S_1^y$ TRANSITION

Figure 5 shows the fluorescence excitation spectrum of H_2P in the range 4660–5100 Å. This spectral range reveals the appearance of the second $S_0 \rightarrow S_1^y$ electronic transition. The intense feature at 5029.1 Å (19884 cm^{-1}) is attributed to the electronic origin of the $S_0 \rightarrow S_1^y$ transition.

Our spectroscopic data provide an accurate determination of the splitting between the electronic origin of the S_1^x and S_1^y states of the isolated H_2P molecule, the electronic energy gap being $\Delta E = 3564 \pm 4$ cm^{-1}. Table V summarizes some of the features of the 0–0 of the second electronic transition. The spectral solvent shifts for the $S_0 \rightarrow S_1^y$ transitions in benzene[11] ($\delta\nu = -682$ cm^{-1}) and in chloromethane[11] ($\delta\nu = -579$ cm^{-1}) are considerably larger than the corresponding spectral solvent shifts for the first $S_0 \rightarrow S_1^x$ transition, e.g., $\delta\nu = -120$ cm^{-1} for benzene[11] (Table I). These large red spectral solvent shifts for the $S_0 \rightarrow S_1^y$ transition of H_2P can readily be understood in terms of dispersive interactions induced by the moderately large oscillator strength

TABLE V. Energetics of the electronic origin of the $S_0 \rightarrow S_1^y$ transition (the Q_y band) of free-base porphine.

Medium	Peak energy (cm^{-1})	Spectral bandwidth (cm^{-1})	Assignment	Reference
Supersonic expansion He	19884	12	0–0 Minor rotational broadening and homogeneous relaxation broadening	Present work
Gas phase 393°C	19550	880	Unresolved vibrational sequence congestion and rotational broadening[a]	11
Ch_2Cl_2 solution 25°C	19305	520	Unresolved vibrational sequence congestion and inhomogeneous broadening[a]	11
Benzene solution 25°C	19201	~500	Unresolved vibrational sequence congestion and inhomogeneous broadening[a]	11

[a]The huge linewidths in the bulb gas phase and in solution contain a minor (~10 cm^{-1}) contribution from homogeneous relaxation broadening.

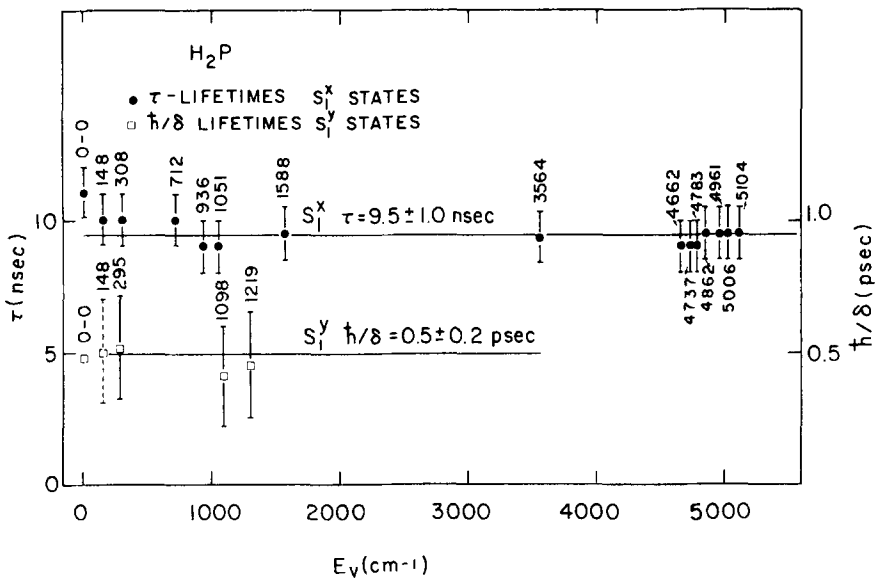

FIG. 6. The dependence of the lifetimes in the S_1^x and S_1^y manifold of isolated H_2P on the excess vibrational energy E_v above the electronic origin of each state. The lifetimes τ in the S_1^x manifold were determined from time-resolved spectroscopy. The lifetimes $\hbar/\delta$ in the S_1^y manifold were estimated from the line broadening of individual, well-resolved, spectral features. The numbers represent the excess vibrational energy above the electronic origin of each state.

($f \simeq 0.06$[11]) for this transition. On the other hand, the oscillator strength for the $S_0 - S_1^x$ transition ($f \simeq 0.01$[11]) is considerably lower, resulting in small dispersive contributions to $\delta\nu$, as discussed in Sec. III. We note in passing that the electronic energy gap between the S_1^y and S_1^x origins is expected to be solvent dependent, as the dispersive contributions to the solvent-induced spectral shifts are different for these two states. Thus, a solvent dependent ΔE does not necessarily reflect the manifestations of solvent-induced configurational change.[11] On the other hand, blue solvent spectral shifts may reflect the spectroscopic manifestation of such "chemical effects," as discussed in Sec. III.

A remarkable general property of the spectral features of the second spin-allowed $S_0 - S_1^y$ transition of the isolated H_2P molecule (Figs. 5 and 6) is the dramatic line broadening of the electronic-vibrational excitations in the S_1^y manifold, whose widths are $\Delta = 10$–15 cm^{-1}, which exceed by about one order of magnitude the rotational broadening $\Delta = 1.0$–1.5 cm^{-1} in the S_1^x manifold. The line broadening in the S_1^y manifold is attributed to the homogeneous broadening, resulting from interstate $S_1^y - S_1^x$ electronic relaxation (Sec. VII). The peak intensity of the electronic origin of S_1^y (Figs. 5 and 6) is roughly comparable (within a large uncertainty of a numerical factor of ~2) to the peak intensity of the electronic origin of S_1^x (Fig. 1), while their widths differ by one order of magnitude. Accordingly, the ratio between the integrated intensities of the electronic origins of $S_0 - S_1^y$ and $S_0 - S_1^x$ is ~10. This very rough estimate is in accord with the experimental estimates of the oscillator strength of solution spectra,[11] i.e., $f \simeq 0.01$ for $S_0 - S_1^x$ and $f \simeq 0.06$ for $S_0 - S_1^y$ and concurs with the large red spectral solvent shift for the $S_0 - S_1^y$ origin. Our conclusion concerning the relative intensity of the electronic origins of the $S_0 - S_1^y$ and $S_0 - S_1^x$ transitions of isolated H_2P seems to be in variance with the analysis of the Leiden group,[10] who concluded that for H_2P in Shpolskii crystals the peak intensity of the $S_0 - S_1^y$ transition is weak. Further work is required to resolve this interesting issue.

The dramatic homogeneous broadening of the spectral features of the $S_0 - S_1^y$ transition (Fig. 5) intrinsically limits the spectral resolution of the vibrational level structure in the S_1^y state. Table VI presents a vibrational analysis of the second electronic transition of the isolated H_2P. There is a good agreement between the energies of the vibrational excitations in the S_1^y and in the S_1^x manifold, which enabled us to assign some fundamentals in the S_1^y manifold. The relative intensities of some of the low vibrational features in the S_1^y manifold are lower than the corresponding vibrational excitations in S_1^x (see Table II and VI). Typical examples are: (i) $I = 9\%$ for the 148 cm^{-1} mode in S_1^y and $I = 30\%$ for the corresponding 148 cm^{-1} vibration in S_1^x. (ii) $I = 12\%$ for the 295 cm^{-1} vibration in S_1^y and $I = 43\%$ for the corresponding 304 cm^{-1} vibration in S_1^x. The simple-minded interpretation of this effect rests on different displacements of the origins of the potential surfaces of S_1^x and S_1^y along some normal coordinates. On the other hand, as the S_1^y origin is closer to the intense Soret band than is the S_1^x origin, one may expect that the Herzberg–Teller vibronic coupling will be more extensive in the S_1^y manifold. The appearance of the 379 and 410 cm^{-1} features may be due to this effect. Furthermore, the lowering of the relative intensities of some of the vibrations in the S_1^y manifold may originate from destructive interference between the allowed component and the vibronically induced component of the transition moment.[20]

VI. ELECTRONIC RELAXATION FROM THE S_1^x STATE

Individual vibrational excitations in the S_1^x manifold at excess vibrational energies $E_v = 0$–1600 cm^{-1} were selectively photoexcited and their decay lifetimes τ were determined by monitoring the time-resolved emission (Fig. 6). The lifetime of the electronic origin of the S_1^x state was found to be $\tau = 11 \pm 1$ ns. The pure radiative lifetime τ_r for the S_1^x state, estimated from the

TABLE VI. Vibrational level structure in the S_1^y state (the Q_y band) of free-base porphine in supersonic expansions of He. Electronic origin of S_1^y at 19 884 cm^{-1}.[a]

S_1^y state			Frequencies in S_1^x state
$\Delta\nu$[b] (cm^{-1})	I[c]	Assignment[d]	$\Delta\nu$ (cm^{-1})
0	100	0–0	
148	9	F	148
295	12	F	304
379	9		
410[e]	10		
773	m	F	783
984	m	F	984
1049	m	F	1049
1098	s		1108
1173	s	F	1162
1219	s	F	1209
1298	w sh		1300
1320	m		1319, 1322
1397	w		1391, 1403
1442	s		1456
1527	w sh		1520, 1527, 1530
1540	s	F	1556

[a]Absolute accuracy of 0–0 position is ±4 cm^{-1}.
[b]$\Delta\nu$—frequencies relative to electronic origin. Accuracy ±2 cm^{-1}.
[c]Relative peak intensity. In the range $\Delta\nu = 0$–410 cm^{-1} I is accurate within ±25%. For the range $\Delta\nu = 750$–1540 cm^{-1} a rough estimate of intensities is given in terms of: s—strong and w—weak, while sh denotes a shoulder.
[d]F—fundamental frequency.
[e]The spectral range corresponding to $\Delta\nu = 450$–750 cm^{-1} was not studied.

integrated oscillator strength, is $\tau_r = 120$ ns, so that $\tau/\tau_r \cong 0.09$ for the electronic origin.

Additional data for the dependence of τ on E_v in the S_1^x manifold was obtained by excitation of states in the S_1^y manifold and interrogation of the radiative decay lifetimes on the nanosecond time scale. The processes involved are

$$S_1^y(v) \xrightarrow{\tau(S_1^y)} S_1^x(E_v) \xrightarrow{\tau} S_0 ,$$

where $S_1^y(v)$ is the initially excited v state in the S_1^y manifold, which decays nonradiatively on the time scale $\tau(S_1^y) = 0.5$ ps (see Sec. VII). The S_1^x state at the excess vibrational energy E_v, produced by internal conversion, is characterized by the lifetime τ, which is experimentally monitored. The lifetimes of some $S_1^x(E_v)$ states in the energy range $E_v = 3564$–5050 cm^{-1} obtained from time-resolved spectroscopy are portrayed in Fig. 6. The independence of τ on E_v in the S_1^x states prevails over a broad range $E_v = 0$–5000 cm^{-1}. This state of affairs corresponds again in the terminology of part I[4] to the case of "total independence", which seems to constitute a universal feature for photoselected vibrational states in the lowest excited singlet states of porphyrins.[4,5]

VII. RADIATIONLESS DECAY OF THE S_1^y STATE

The energy gap between the electronic origins of the S_1^y and S_1^x states is 3564 cm^{-1}. Although this energy gap is quite modest, the density of vibrational states of the S_1^x manifold, which are quasidegenerate with the low-lying S_1^y levels, is large for this huge molecule. We shall provide spectroscopic evidence that the S_1^y–S_1^x interstate coupling corresponds to the statistical limit. Quantitative information on the time scale for electronic relaxation from the S_1^y state will be obtained.

A cursory comparison between the spectral features of the $S_0 \rightarrow S_1^x$ transition (Fig. 1) and of the $S_0 \rightarrow S_1^y$ tran-

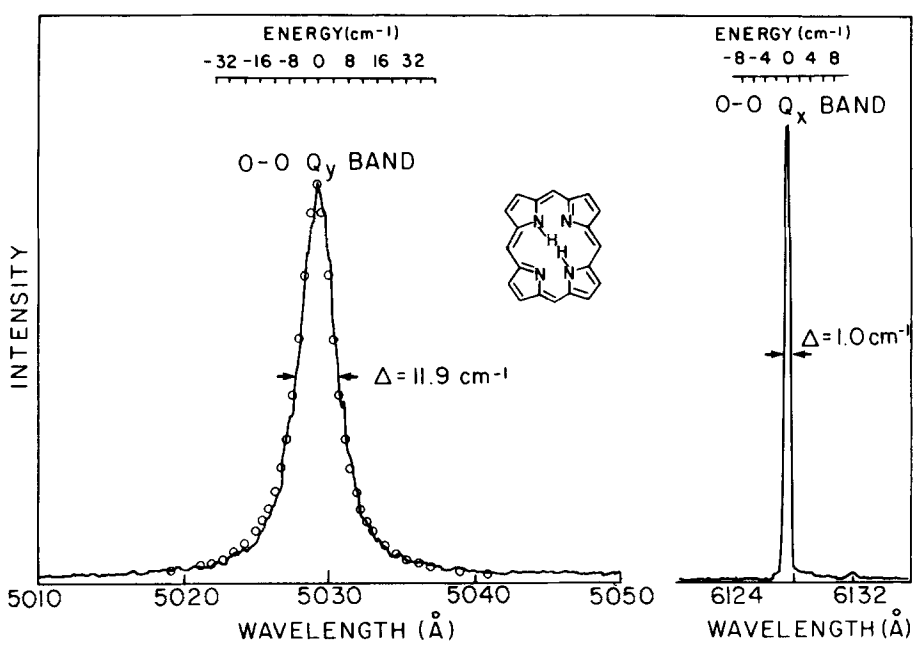

FIG. 7. The electronic origins of the $S_0 \rightarrow S_1^x$ and of the $S_0 \rightarrow S_1^y$ transitions of H_2P in seeded supersonic expansions of He. Experimental conditions as in Fig. 1. Solid lines represent the experimental spectra. Circles correspond to the fit of the 0–0 of the $S_0 \rightarrow S_1^y$ transition to a Lorentzian line shape.

sition (Fig. 5) reveals a dramatic line broadening of the electronic-vibrational excitations in the S_1^y manifold. In Fig. 7 we portray the electronic origins of the S_1^x and S_1^y states. The linewidth of the S_1^x origin is $\Delta = 1.0$ cm^{-1}, originating from rotational broadening, while the linewidth of S_1^y is $\Delta = 11.9$ cm^{-1}, being larger by one order of magnitude than Δ of S_1^x. This line broadening of the S_1^y origin and of its higher vibrational excitations is attributed to interstates of $S_1^y - S_1^x$ coupling. From Fig. 7 it is apparent that the line shape of the broadened S_1^y origin is smooth and does not reveal any fine structure. Accordingly, the $S_1^y - S_1^x$ coupling in H_2P corresponds to the statistical limit[21] rather than to the intermediate level structure. It is apparent that the electronic energy gap in this huge molecule is sufficiently large to warrant statistical coupling.

Invoking the reasonable assumption that rotational line broadening in the S_1^x and S_1^y states is practically identical, we can assert that rotational broadening effects in S_1^y amount to 10% of Δ for this state and are thus negligible. We can then proceed to explore the line shape of the S_1^y excitations. In Fig. 7 we demonstrate that the line shape of the S_1^y origin is Lorentzian. Accordingly, the linewidth $\Delta = 11.9$ cm^{-1} of $S_1^y(0)$ can be attributed to homogeneous broadening due to the $S_1^y \rightarrow S_1^x$ decay. This quantitative observation of homogeneous "lifetime broadening" in the statistical limit within a bound level structure of a large "isolated" molecule is of considerable interest as the spectroscopic implications of the statistical limit were not explored previously in isolated, ultracold, large molecules. From the practical point of view, quantitative information can be inferred concerning lifetimes for the ultrafast, electronic relaxation process. The lifetime of the electronic origin of S_1^y is $\tau = \hbar/\Delta = 5 \times 10^{-13}$ s, providing a reliable spectroscopic determination of the subpicosecond time scale for intramolecular electronic relaxation of an individual electronic excitation in a large isolated molecule.

Information on the lifetimes of individual vibrational excitations in the S_1^y manifold was obtained from line-broadening data of Fig. 5. We have selected for this analysis several vibrational excitations in S_1^y, which are well separated from neighboring spectral features. The widths δ of these vibrational states in the range $E_v = 0-1500$ cm^{-1} above the electronic origins of S_1^y are $\delta = 10-15$ cm^{-1}. These values of δ, which considerably exceed the rotational inhomogeneous broadening, are attributed to homogeneous broadening originating from electronic relaxation. The lifetimes $\tau = \hbar/\delta$ for the electronic excitations in the S_1^y manifold (Fig. 6) are practically independent of E_v. This total independence of τ on E_v, which is inferred from energy-resolved spectroscopy for the S_1^y state, is analogous to the independence of τ on E_v in the S_1^x manifold.

The radiationless $S_1^y \rightarrow S_1^x$ electronic relaxation in H_2P may be unique, involving a photochemical process due to the rotation of the H–H axis.[8,21] Our spectroscopic relaxation data cannot establish at present whether this photochemical transformation contributes directly to the homogeneous line broadening or, rather, whether it occurs from the vibrationally hot S_1^x manifold produced via internal conversion. Spectroscopic studies of photochemical transformations in large, isolated, ultracold molecules in supersonic expansions will open up a novel and challenging research area.

ACKNOWLEDGMENT

This research was supported by the United States Army through its European Research Office.

[1] U. Even, J. Magen, J. Jortner, and H. Levanon, J. Am. Chem. Soc. **103**, 4583 (1981).
[2] U. Even, J. Magen, and J. Jortner, Chem. Phys. Lett. **88**, 131 (1982).
[3] U. Even, J. Jortner, and J. Friedman, J. Phys. Chem. 86, 2273 (1982).
[4] U. Even, J. Magen, J. Jortner, J. Friedman, and H. Levanon, J. Chem. Phys. **77**, 4374 (1982).
[5] U. Even, J. Magen, J. Jortner, and J. Friedman, J. Chem. Phys. **77**, 4384 (1982).
[6] U. Even, J. Magen, J. Jortner, and H. Levanon, J. Chem. Phys. **76**, 5684 (1982).
[7] M. Gouterman, in *The Porphyrins*, edited by D. Dolphin (Academic, New York, 1978), Vol. III, p. 1.
[8] S. Voelker and J. H. van der Waals, Mol. Phys. **32**, 1703 (1976).
[9] S. Voelker and R. M. MacFarlane, Chem. Phys. Lett. **61**, 421 (1979).
[10] A. I. M. Dicker, M. Noort, S. Voelker, and J. H. van der Waals, Chem. Phys. Lett. **73**, 1 (1980).
[11] L. Edwards, D. H. Dolphin, M. Gouterman, and A. D. Adler, J. Mol. Spectrosc. **38**, 16 (1971).
[12] U. Even and J. Jortner (unpublished).
[13] J. A. Mullins, A. D. Adler, and R. M. Hochstrasser, J. Chem. Phys. **43**, 2578 (1965).
[14] L. Edwards and M. Gouterman, J. Mol. Spectrosc. **33**, 292 (1970).
[15] L. Edwards, D. H. Dolphin, and M. Gouterman, J. Mol. Spectrosc. **35**, 90 (1970).
[16] S. H. Fitch, C. A. Hayman, and D. H. Levy, J. Chem. Phys. **73**, 1064 (1980).
[17] J. A. Pople and H. C. Longuet-Higgins, J. Chem. Phys. **27**, 192 (1957).
[18] U. Even, A. Amirav, S. Leutwyler, M. J. Ondrechen, Z. Berkovitch-Yellin, and J. Jortner, Discussion No. 73, Faraday Society (London) 1982.
[19] S. Voelker and R. M. MacFarlane, J. Chem. Phys. **73**, 4476 (1980).
[20] D. P. Craig and G. J. Small, J. Chem. Phys. **49**, 3827 (1969).
[21] M. Gouterman and L. Stryer, J. Chem. Phys. **37**, 2260 (1962).